Journal of Power Sources, 39 (1992) 285–297

Cell performance of molten-carbonate fuel cell with alkali and alkaline-earth carbonate mixtures

Kazumi Tanimoto*, Yoshinori Miyazaki, Masahiro Yanagida, Shigeo Tanase, Toshikatsu Kojima, Norikazu Ohtori, Hironobu Okuyama and Teruo Kodama
Government Industrial Research Institute, Osaka Midorigaoka 1-8-31, Ikeda, Osaka 563 (Japan)

(Received March 26, 1992)

Abstract

Molten-carbonate fuel cells with two types of alkali carbonate mixture as the electrolyte have been operated. The resulting cell performances have been compared in order to optimize the composition of each carbonate mixture. One electrolyte type is a mixture of the high lithium eutectic ($(Li_{0.62}K_{0.38})_2CO_3$) and an alkaline-earth carbonate, while the other is a mixture of the lithium–sodium eutectic ($(Li_{0.52}Na_{0.48})_2CO_3$) and an alkaline-earth carbonate. Additions of $CaCO_3$, $SrCO_3$ and $BaCO_3$ have been used. A small amount of each alkaline-earth carbonate to both eutectics does not influence the cell performance. On the other hand, larger amounts reduce the cell performance. The required content of each additive to provide optimum cell performance depends on both the additive itself and the host eutectic. The temperature dependence of cell performance in the presence of the different additives has also been investigated. There is little difference between the behaviour of $((Li_{0.62}K_{0.38}K_{0.38})_2–Ca)CO_3$, $((Li_{0.62}K_{0.38})_2–Ba)CO_3$ and $((Li_{0.52}Na_{0.48})_2–Ca)CO_3$. By contrast, high temperature dependence was found for $((Li_{0.62}K_{0.38})_2–Sr)CO_3$, $((Li_{0.52}Na_{0.48})_2–Sr)CO_3$ and $((Li_{0.52}Na_{0.48})_2–Ba)CO_3$.

Introduction

Addition of alkaline-earth carbonate to alkali carbonate mixtures that serve as the electrolyte for a molten-carbonate fuel cell (MCFC) offers the prospect of an improvement in the endurance of the system. The alkaline-earth carbonate effectively reduces the solubility of the nickel oxide cathode into the carbonate mixture [1]. In this respect, a high lithium eutectic, $(Li_{0.62}K_{0.38})_2CO_3$, is typically used.

The dissolution of nickel oxide (which is typically used as the cathode material) in the carbonate mixture is one of the factors that limit the long-time operation of MCFCs. The degradation of the cathode gives rise to a short-circuit in the electrolyte. This is due to reprecipitation of the dissolved nickel. To elucidate the dissolution behaviour of the nickel oxide, both Orfield and Shores [2] and Ota *et al.* [3] have measured the solubility of nickel oxide in carbonate mixtures and have investigated the mechanism of the process. Two procedures have been suggested to overcome the problem: (i) the use of alternative cathode materials, e.g., $LiFeO_2$ [4]; (ii) the optimization of carbonate composition to provide a milder environment for the nickel oxide cathode.

*Author to whom correspondence should be addressed.

0378-7753/92/$5.00

With respect to optimization of carbonate composition, Ota *et al.* [3] pointed out that the solubility of nickel oxide in $(Li_{0.52}Na_{0.48})_2CO_3$ was lower than that in $(Li_{0.62}K_{0.38})_2CO_3$. In other work, Doyon *et al.* [5] suggested that the addition of MgO, CaO and SrO to $(Li_{0.62}K_{0.38})_2CO_3$ reduced the solubility of nickel oxide. We further reported [1] that the addition of alkaline-earth carbonate to $(Li_{0.62}K_{0.38})_2CO_3$ reduced the solubility of nickel oxide. Finally, Shores *et al.* [6] found that the addition of alkaline-earth carbonate to $(Li_{0.62}K_{0.38})_2CO_3$ gave similar behaviour.

From laboratory-scale cell testing with various carbonate mixtures, Kishida [7] observed that the addition of 1 mol.% of an alkaline-earth cation to $(Li_{0.62}K_{0.38})_2CO_3$ caused 50% reduction in the amount of dissolved nickel. Ogawa *et al.* [8] also employed a laboratory-scale cell containing the carbonate mixture with additives, $CaCO_3$, $SrCO_3$ and $BaCO_3$, and after 2000 or 3000 h of operation there was a reduction in the amount of nickel dissolved in the carbonate mixtures. It was suggested that alkaline-earth cations prevented nickel cations from diffusing to the anode side. The studies of Veldhuis *et al.* [9] corroborated these results.

Although the addition of alkaline-earth carbonate to $(Li_{0.62}K_{0.38})_2CO_3$ almost certainly impedes the dissolution of nickel oxide, the influence of the content of alkaline-earth carbonate on cell performance has still to be determined. Furthermore, the effect of alkaline-earth carbonate additions to $(Li_{0.52}Na_{0.48})_2CO_3$ has not been examined by laboratory-scale cell testing. Accordingly, the work, reported here, describes the initial cell performance of laboratory-scale cells in which various contents of the alkaline-earth carbonates $CaCO_3$, $SrCO_3$ and $BaCO_3$ are added to the eutectic carbonate mixtures $(Li_{0.62}K_{0.38})_2CO_3$ and $(Li_{0.52}Na_{0.48})_2CO_3$ at various temperatures.

Experimental

The matrix and carbonate-mixture tapes were fabricated independently [10]. A small piece of green matrix tape was fired at 500 °C for 3 h and then the pore volume per weight was measured at room temperature by mercury intrusion porosimetry. The porosity was calculated from this value and taking the density of γ-$LiAlO_2$ as 2.610 g cm^{-3} [10]. The porosity was found to be 65%. The weight of the green matrix tape corresponded to the pore volume after burnout. The characteristics of the tested carbonate mixtures are given in Table 1. The volume of the carbonate mixture was calculated from the weight of the green tape and its density at room temperature. The electrolyte loading ratio (ELR) was defined as follows:

$$ELR = V_{\text{carbonate mixture}}/V_{\text{matrix pore}} \quad (1)$$

where $V_{\text{carbonate mixture}}$ is the volume of the carbonate mixture and $V_{\text{matrix pore}}$ is the pore volume, both at room temperature. The amount of the carbonate mixture in the green tape was adjusted according to the ELR to provide a good cell performance.

The test cell comprised an anode (35 mm diameter, 0.8 mm thickness), a cathode (35 mm diameter, 0.4 mm thickness), green matrix tape (50 mm diameter, 0.6 mm thickness), green carbonate mixture tape, and support frames. The anode was a Ni–10 wt.% Cr porous plaque and the cathode a Ni porous plaque. The latter was oxidized *in situ* to NiO. Both electrodes were obtained from Imperial Clevite Co. (Cleveland, OH, USA). The effective surface area of the electrodes was 10 cm^2. The cell frame was constructed from SUS316L steel.

The assembled test cell was heated to 450 °C and held at for 3 h with air flowing through both anode and cathode to burn out the organic binder, etc. After burnout,

TABLE 1

Characteristics of carbonate mixtures

Mixture	Composition	Density ($g\ cm^{-3}$)	Optimum electrolyte loading ratio (%)
Li_2CO_3/K_2CO_3	62/38	2.27	100
$Li_2CO_3/K_2CO_3/CaCO_3$	62/3810	2.11	130
$Li_2CO_3/K_2CO_3/CaCO_3$	62/38/20	1.97	130
$Li_2CO_3/K_2CO_3/CaCO_3$	62/38/30	1.85	130
$Li_2CO_3/K_2CO_3/SrCO_3$	62/38/5	2.17	120
$Li_2CO_3/K_2CO_3/SrCO_3$	62/38/10	2.09	100
$Li_2CO_3/K_2CO_3/SrCO_3$	62/38/20	1.93	120
$Li_2CO_3/K_2CO_3/BaCO_3$	62/38/10	2.07	120
$Li_2CO_3/K_2CO_3/BaCO_3$	62/38/20	1.90	120
Li_2CO_3/Na_2CO_3	52/48	2.33	110–130
$Li_2CO_3/Na_2CO_3/CaCO_3$	52/48/5	2.26	110
$Li_2CO_3/Na_2CO_3/CaCO_3$	52/48/10	2.15	110
$Li_2CO_3/Na_2CO_3/SrCO_3$	52/48/5	2.22	110
$Li_2CO_3/Na_2CO_3/SrCO_3$	52/48/10	2.12	110
$Li_2CO_3/Na_2CO_3/BaCO_3$	52/48/5	2.21	110
$Li_2CO_3/Na_2CO_3/BaCO_3$	52/48/10	2.10	110

carbon dioxide was introduced into the anode and cathode, and the system heated to 650 °C. At this stage, fuel gas ($H_2/CO_2 = 80/20$ vol.%) and oxidant gas ($O_2/CO_2 = 33/67$ vol.%) were introduced into the anode and cathode, respectively. The flow rate into the anode and cathode was 70 and 90 ml min^{-1}, respectively. Each gas utilization corresponded to 20% at 150 mA cm^{-2}.

The cell was operated under a load of 150 mA cm^{-2} until the performance became stable. This took about 50 to 100 h. Under stable conditions, the cell voltage at 0, 50, 100, 150 and 200 mA cm^{-2} was measured (with the constant gas flow given above) at increasing temperatures between 600 and 700 °C. The cell resistance was measured under a load of 100 mA cm^{-2} by a current-interrupt method. The cells were operated for up to 200 h. After testing, it was found that each carbonate mixture was impregnated uniformly into the matrix tape.

Results and discussion

Optimization of electrolyte loading ratio (ELR)

For $(Li_{0.62}K_{0.38})_2CO_3$ electrolyte, the relationship between *ELR* and cell voltage at 150 mA cm^{-2} is shown in Fig. 1. The best cell voltage was obtained at ELR = 100%, For all the carbonate mixtures values of ELR in the range 90 to 140% were examined. The optimum values of ELR are given in Table 1. In general, the optimum ELRs of $((Li_{0.62}K_{0.38})_2$–AE)CO_3 mixtures are larger than those of $((Li_{0.52}Na_{0.48})_2$–AE)CO_3 mixtures*. The density of $(Li_{0.62}K_{0.38})_2CO_3$ at room temperature and the typical operating temperature of 650 °C is 2.26 and 1.93 g cm^{-3}, respectively [11]. The corresponding density for $(Li_{0.52}Na_{0.48})_2CO_3$ is 2.33 and 1.96 g cm^{-3} [11]. The ratio of the volume

*In this paper, AE is used to denote the alkaline-earth metal.

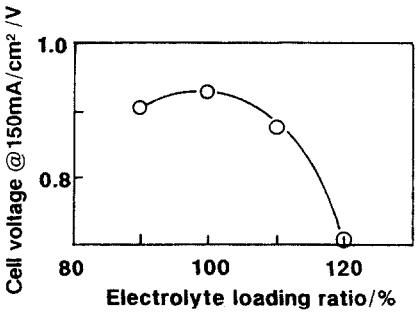

Fig. 1. (Cell voltage (IR included) at 150 mA cm^{-2} vs. ELR for $(Li_{0.62}K_{0.38})_2CO_3$ eutectic.

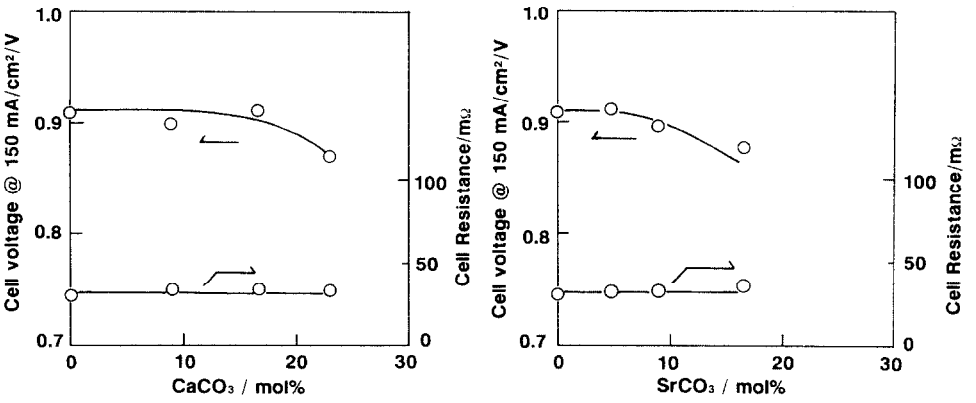

Fig. 2. Cell voltage (IR and ohmic resistance included) at 150 mA cm^{-2} vs. calcium carbonate content in $(Li_{0.62}K_{0.38})_2CO_3$ eutectic.

Fig. 3. Cell voltage (IR and ohmic resistance included) at 150 mA cm^{-2} vs. strontium carbonate content in $(Li_{0.62}K_{0.38})_2CO_3$ eutectic.

at room temperature to that at 650 °C is 85.5 and 84.0% for $(Li_{0.62}K_{0.38})_2CO_3$ and $(Li_{0.52}Na_{0.48})_2CO_3$, respectively. The difference in these values is not significant. By contrast, the difference in the optimum ELRs for $(Li_{0.62}K_{0.38})_2CO_3$ and $(Li_{0.52}Na_{0.48})_2CO_3$ is thought to be due to a change in the wettability of the carbonate on the electrode.

Cell performance with additives

The relationship between the amount of added alkaline-earth carbonate and cell voltage under a loading of 150 mA cm^{-2} at the optimum ELR are presented in Figs. 2 to 7. The cell voltage includes the ohmic and Nernst losses. It can be seen that the cell voltage is reduced when large amounts of alkaline-earth carbonate are added. The range of additive concentration over which the cell voltage remains invariant is referred to as the 'insensitive region'. The regions for the various additives in each of the carbonate mixtures are given in Table 2. The voltage of test cells with additives in the insensitive region was similar to that for cells without additives. The widest insensitive region was exhibited by $((Li_{0.62}K_{0.38})_2\text{–}Ca)CO_3$, whilst the narrowest region (<10 mol.%) was observed with $((Li_{0.62}K_{0.38})_2\text{–}Sr)CO_3$. The insensitive regions of $((Li_{0.52}Na_{0.48})_2\text{–}AE)CO_3$ were narrower than those of $((Li_{0.62}K_{0.38})_2\text{–}AE)CO_3$. The in-

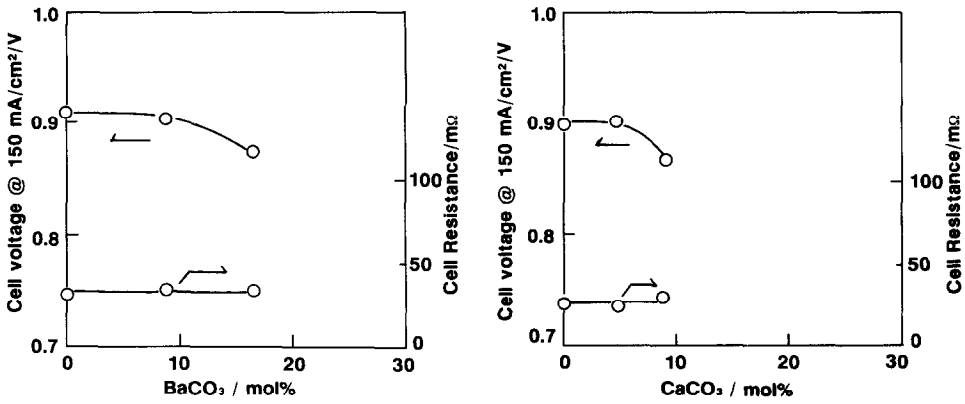

Fig. 4. Cell voltage (IR and ohmic resistance included) at 150 mA cm^{-2} vs. barium carbonate content in $(Li_{0.62}K_{0.38})_2CO_3$ eutectic.

Fig. 5. Cell voltage (IR and ohmic resistance included) at 150 mA cm^{-2} vs. calcium carbonate content in $(Li_{0.52}Na_{0.48})_2CO_3$ eutectic.

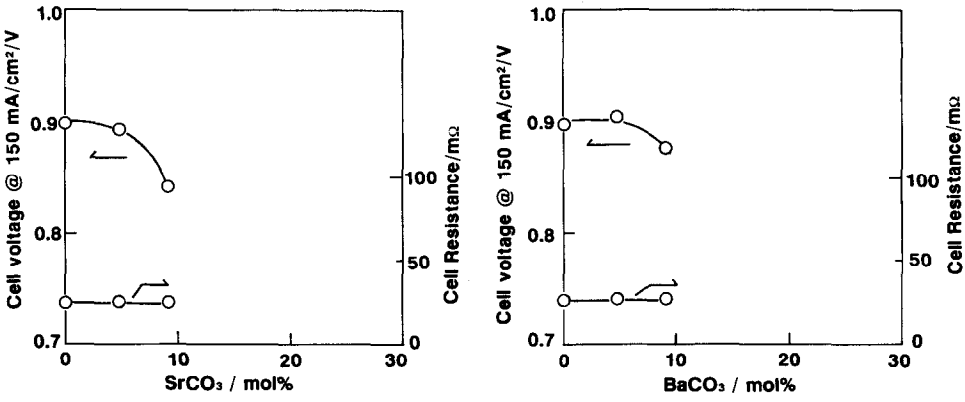

Fig. 6. Cell voltage (IR and ohmic resistance included) at 150 mA cm^{-2} vs. strontium carbonate content in $(Li_{0.52}Na_{0.48})_2CO_3$ eutectic.

Fig. 7. Cell voltage (IR and ohmic resistance included) at 150 mA cm^{-2} vs. barium carbonate content in $(Li_{0.52}Na_{0.48})_2CO_3$ eutectic.

TABLE 2

The insensitive region of various additives in carbonate electrolytes

Carbonate electrolyte	Insensitive region (mol.%)		
	$CaCO_3$	$SrCO_3$	$BaCO_3$
$(Li_{0.62}K_{0.38})_2CO_3$	0–15	0–5	0–10
$(Li_{0.52}Na_{0.48})_2CO_3$	0–5	0–5	0–5

flection points of the performance curves for a test cell with $(Li_{0.52}Na_{0.48})_2CO_3$ and the additives were <5 mol.%.

Although a high content of additive in either $(Li_{0.62}K_{0.38})_2CO_3$ or $(Li_{0.52}Na_{0.48})_2CO_3$ reduced the cell voltage, there was no change in the cell resistance. The resistance with $((Li_{0.62}K_{0.38})_2$–AE$)CO_3$ was slightly higher, about 5 mΩ, than that with $((Li_{0.52}Na_{0.48})_2$–AE$)CO_3$. This was due to a difference in the electrical conductivity of the two carbonate mixtures, viz., 1.98 and 1.23 S cm^{-1} at 650 °C for $(Li_{0.52}Na_{0.48})_2CO_3$ and $(Li_{0.62}K_{0.38})_2CO_3$, respectively [12]. Since the effect of additions of alkaline-earth carbonate to $(Li_{0.62}K_{0.38})_2CO_3$ and $(Li_{0.52}Na_{0.48})_2CO_3$ on the electrical conductivity was low, there was little change to the cell resistance of either $((Li_{0.62}K_{0.38})_2$–AE$)CO_3$ or $((Li_{0.52}Na_{0.48})_2$–AE$)CO_3$. The reduction in cell voltage beyond the insensitive region is not due to cell-resistance effects but rather to the kinetics of the process in molten-carbonate mixtures. In particular, the basicity of the carbonate is considered to be an important factor.

As stated above, the solubility of nickel oxide is lower in $(Li_{0.52}Na_{0.48})_2CO_3$ than in $(Li_{0.62}K_{0.38})_2CO_3$. It is expected that $((Li_{0.52}Na_{0.48})_2$–AE$)CO_3$ is a very favourable mixture for lowering the dissolution of nickel. Further, it was reported that the addition of alkaline-earth carbonate to $(Li_{0.62}K_{0.38})_2CO_3$ reduced the dissolution of nickel oxide into the carbonate mixture. In the insensitive region, there was no decrease in the cell voltage on the addition of alkaline-earth carbonate. Considering the low solubility of nickel oxide, a small amount of alkaline-earth carbonate in $(Li_{0.62}K_{0.38})_2CO_3$ or $(Li_{0.52}Na_{0.48})_2CO_3$ provided an effective optimization of the carbonate mixture composition.

Temperature dependence of cell performance

For $((Li_{0.62}K_{0.38})_2$–AE$)CO_3$ and $((Li_{0.52}Na_{0.48})_2$–AE$)CO_3$, the cell voltages at 150 mA cm^{-2} containing the Nernst and ohmic polarization are plotted as a function of temperature in Figs. 8 to 13. The temperature dependence of the cell resistance was not as large as that of the cell voltage in both $((Li_{0.62}K_{0.38})_2$–AE$)CO_3$ and $((Li_{0.52}Na_{0.48})_2$–AE$)CO_3$. The temperature dependence of the cell voltage was due mainly to that of the cell performance. The performance behaviour of the cell in the presence of additives depended on the nature of the individual additive rather than on the carbonate mixture itself. The temperature dependence was highest for $((Li_{0.62}K_{0.38})_2$–Sr$)CO_3$ and $((Li_{0.52}Na_{0.48})_2$–Sr$)CO_3$.

To illustrate the temperature dependence of cell performance, an Arrhenius plot of the inverse of polarization resistance ($1/R_p$) without the Nernst loss and ohmic resistance in $(Li_{0.62}K_{0.38})_2CO_3$ is shown in Fig. 14. The method used to estimate the Nernst loss at each temperature is outlined in the Appendix. The apparent activation energy of the combined cathode and anode reactions for each carbonate composition was derived from the slope of the corresponding Arrhenius plot. The apparent activation energies of $((Li_{0.62}K_{0.38})_2$–Ca$)CO_3$ and $((Li_{0.62}K_{0.38})_2$–Ba$)CO_3$ were not appreciably different from that measured in the absence of additive (see Fig. 15). On the other hand, a larger energy was found in$((Li_{0.62}K_{0.38})_2$–Sr$)CO_3$. The temperature-dependence behaviour of $((Li_{0.52}Na_{0.48})_2$–Sr$)CO_3$ was different from that of $((Li_{0.52}Na_{0.48})_2$–Ca$)CO_3$ (see Fig. 16). The apparent activation energy of the latter was similar to that observed in the non-additive case. The apparent activation energy for the addition of 9 mol.% of $SrCO_3$ to $(Li_{0.52}Na_{0.48})_2CO_3$ was not obtained exactly because of the large experimental deviation. A carbonate mixture of 4 mol.% $BaCO_3$ and $(Li_{0.52}Na_{0.48})_2CO_3$ provided a high apparent activation energy. The latter increased with $BaCO_3$ content. This behaviour

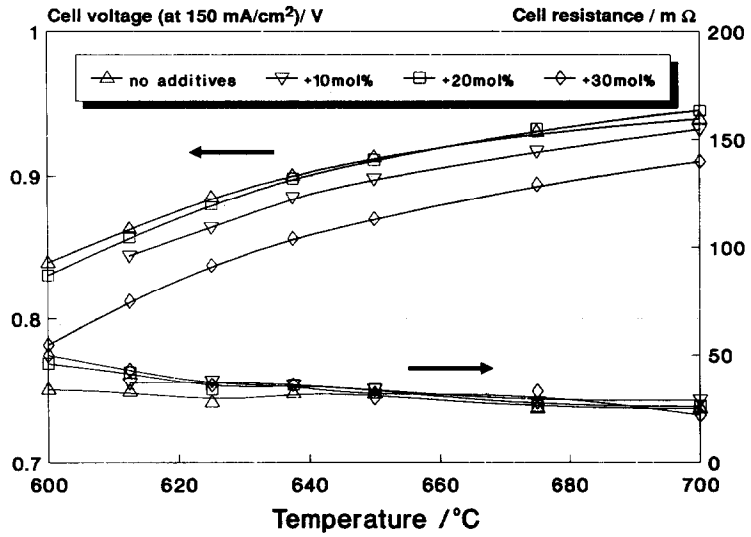

Fig. 8. Cell voltage (IR and ohmic resistance included) at 150 mA cm^{-2} vs. temperature for $((Li_{0.62}K_{0.38})_2$–Ca)CO_3 system.

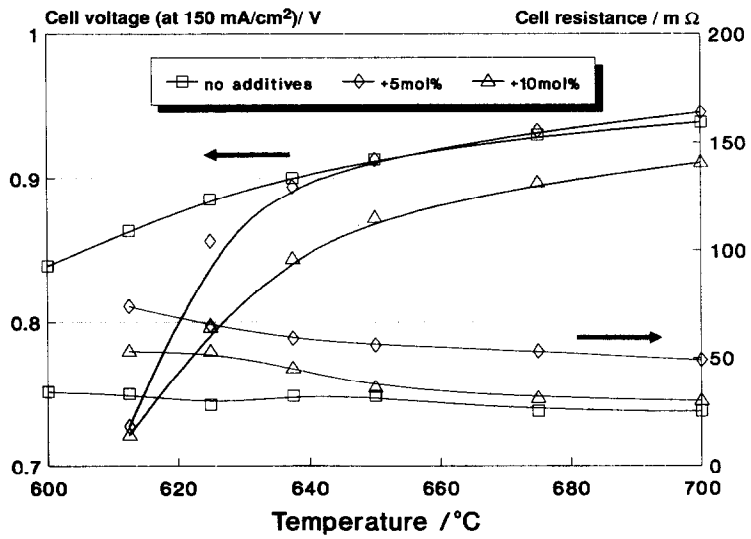

Fig. 9. Cell voltage (IR and ohmic resistance included) at 150 mA cm^{-2} vs. temperature for $((Li_{0.62}K_{0.38})_2$–Sr)CO_3 system.

was similar to that exhibited by $((Li_{0.52}Na_{0.48})_2$–Sr)CO_3. It was found that the behaviour of $((Li_{0.62}K_{0.38})_2$–Sr)CO_3, $((Li_{0.52}Na_{0.48})_2$–Sr)CO_3 and $((Li_{0.52}Na_{0.48})_2$–Ba)CO_3 was very different from that of the other systems. Although a full explanation is not yet available, it is thought that the behaviour, as well as the reduction in cell voltage beyond the insensitive region, are related to the basicity of the carbonate mixtures.

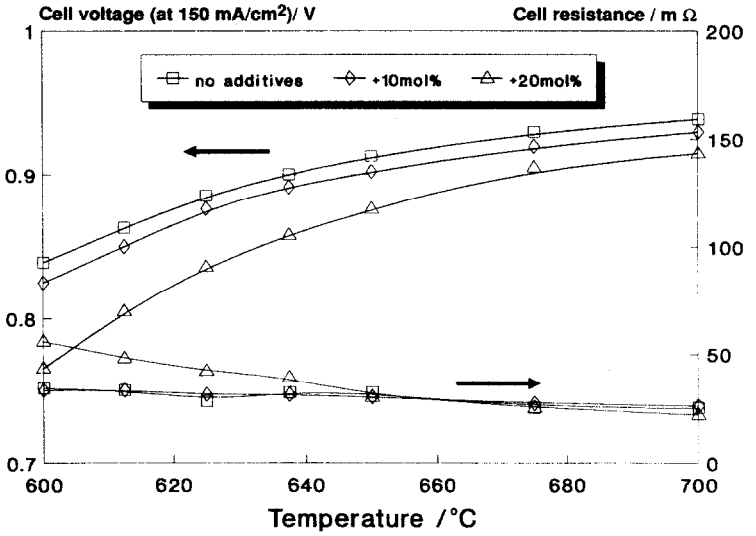

Fig. 10. Cell voltage (IR and ohmic resistance included) at 150 mA cm^{-2} vs. temperature for $((Li_{0.62}K_{0.38})_2$–$Ba)CO_3$ system.

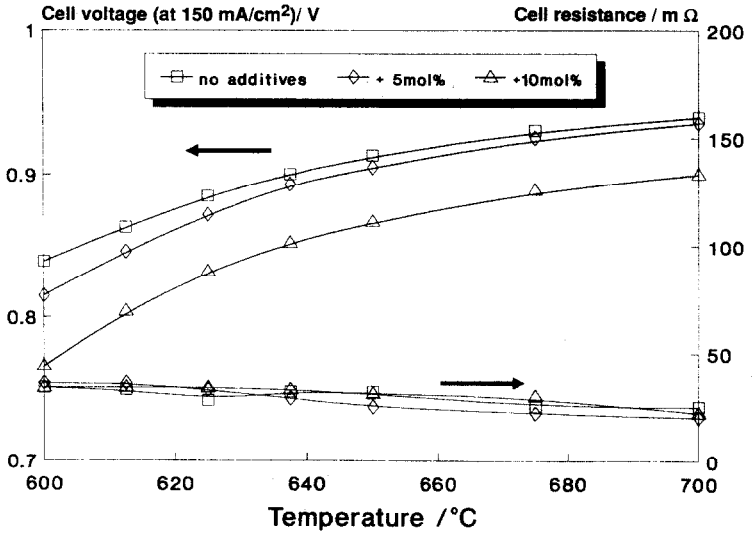

Fig. 11. Cell voltage (IR and ohmic resistance included) at 150 mA cm^{-2} vs. temperature for $((Li_{0.52}Na_{0.48})_2$–$Ca)CO_3$ system.

For the application of alternative carbonate mixtures to MCFCs, it is favourable to achieve a low temperature dependence. In other words, deviations in cell performance brought about by temperature changes should be minimized in large-cell

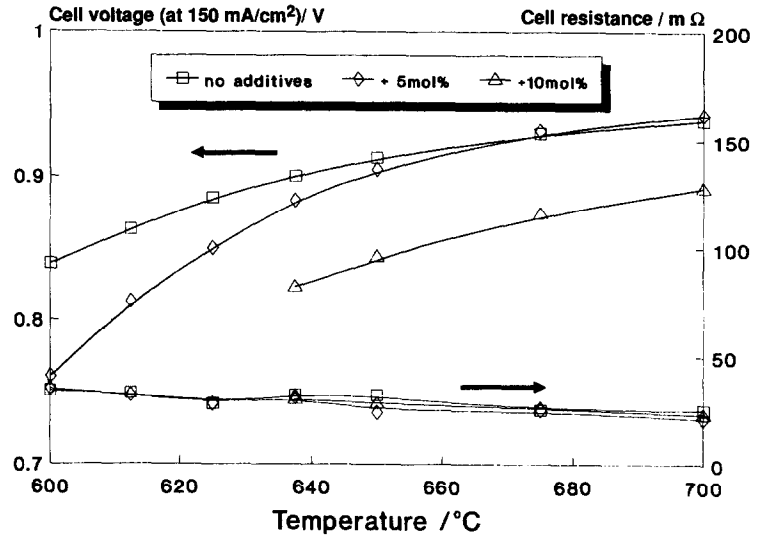

Fig. 12. Cell voltage (IR and ohmic resistance included) at 150 mA cm^{-2} vs. temperature for $((Li_{0.52}Na_{0.48})_2$–Sr)CO_3 system.

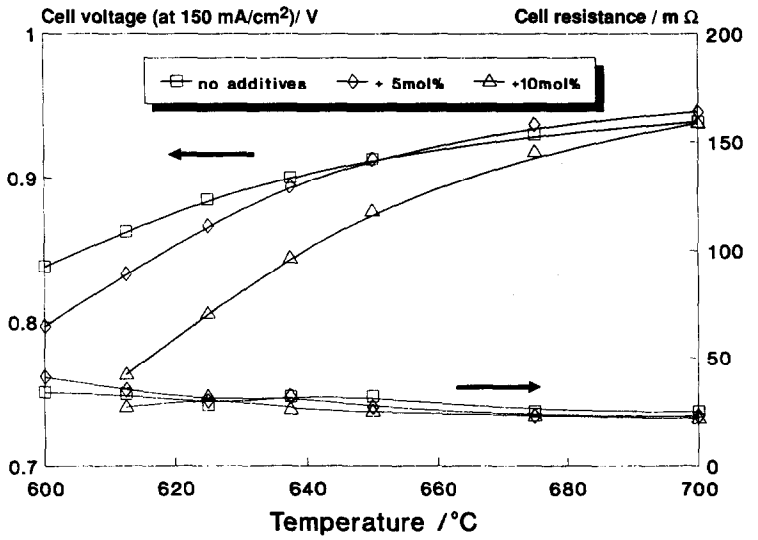

Fig. 13. Cell voltage (IR and ohmic resistance included) at 150 mA cm^{-2} vs. temperature for $((Li_{0.52}Na_{0.48})_2$–Ba)CO_3 system.

operations. From this viewpoint, the insensitive regions of the $((Li_{0.62}K_{0.38})_2$–Ca)CO_3, $((Li_{0.62}K_{0.38})_2$–Ba)CO_3 and $((Li_{0.52}Na_{0.48})_2$–Ca)CO_3 are promising systems for application in MCFCs.

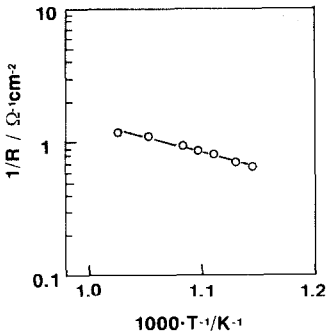

Fig. 14. Arrhenius plot of the inverse of the polarization resistance for $(Li_{0.62}K_{0.38})_2CO_3$ eutectic

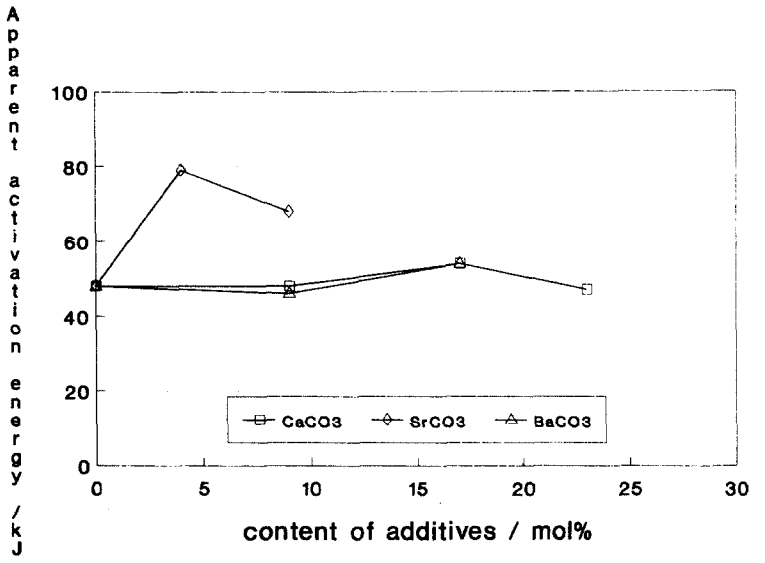

Fig. 15. Apparent activation energy for $((Li_{0.62}K_{0.38})_2$–AE)CO_3 system as a function of alkaline earth (AE) content.

Conclusions

A laboratory-scale (10 cm^2) cell, in which an alkaline-earth carbonate ($CaCO_3$, $SrCO_3$ or $BaCO_3$ is added to either $(Li_{0.62}K_{0.38})_2CO_3$ or $(Li_{0.52}Na_{0.48})_2CO_3$, has been operated for 100 to 200 h. The following observations have been made:

(i) A small amount of alkaline-earth carbonate in $(Li_{0.62}K_{0.38})_2CO_3$ or $(Li_{0.52}Na_{0.48})_2CO_3$ causes no significant decline in cell performance, whereas a large concentration reduces the cell performance.

(ii) For $((Li_{0.62}K_{0.38})_2$–Ca)CO_3, $((Li_{0.62}K_{0.38})_2$–Ba)CO_3 and $((Li_{0.52}Na_{0.48})_2$–Ca)CO_3, there is no significant difference in the temperature dependence of the cell. The apparent activation energy in each carbonate was 50 to 60 kJ mol^{-1}. The highest

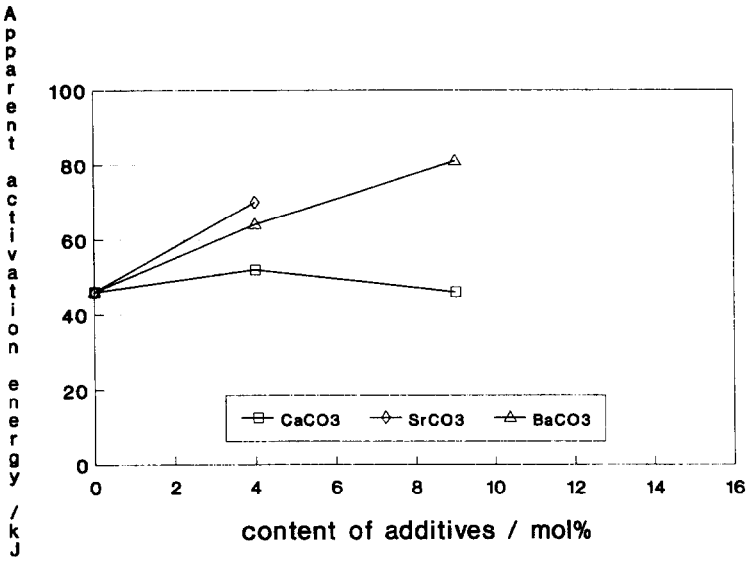

Fig. 16. Apparent activation energy for $((Li_{0.52}Na_{0.48})_2$–AE)CO_3 system as a function of alkaline-earth (AE) content.

temperature dependence was observed for $((Li_{0.62}K_{0.38})_2$–Sr)CO_3 and $((Li_{0.52}Na_{0.48})_2$–Sr)CO_3. By contrast, $((Li_{0.52}Na_{0.48})_2$–Ba)CO_3 exhibits little temperature dependence.

(iii) Considering the above two points, it is suggested that the insensitive regions of $((Li_{0.62}K_{0.38})_2$–Ca)CO_3, $((Li_{0.62}K_{0.38})_2$–Ba)CO_3 and $((Li_{0.52}Na_{0.48})_2$–Ca)CO_3 are promising electrolyte systems for MCFCs.

Appendix

Procedure of analysis of polarization effects

The slope of the polarization curve involves the sum of kinetic, concentration and ohmic components. The polarization curve for a constant inlet flow contains a 'Nernst loss'. Under such conditions, the utilization of fuel gas increases with increasing current density. The equilibrium potential of the anode will shift to the cathodic side due to the consumption of fuel gas. In this work, the cathode potential remained constant as there was no change in gas composition because this was $O_2/CO_2 =$ 33/67 vol.% and gas was consumed in the same ratio, i.e., $O_2/CO_2 = 1/2$. The loss of cell voltage due to the change in fuel-gas composition was estimated from the cell voltage at the inlet and the outlet as follows:

$$\text{Nernst loss} = \frac{(\text{inlet voltage}) - (\text{outlet voltage})}{2} \tag{2}$$

The cell voltage was formulated as follows:

TABLE 3

Open-circuit voltage and Nernst loss under constant gas flow at different temperatures (fuel utilization = 20%, load = 150 mA cm^{-2})

	Temperature (K)						
	873	885	898	911	923	948	973
OCV (mV)	1135	1134	1132	1131	1129	1127	1124
Nernst loss (mV)	26	27	27	28	29	30	33

$$E = E_0 + \frac{RT}{2F} \ln \frac{P_{H_2}}{P_{CO_2} P_{H_2O}} + \frac{RT}{4F} \ln P_{CO_2} P_{O_2}^{1/2} \tag{3}$$

where E, E_0, R, T, F and P_X ($X = H_2$, CO_2, H_2O, O_2) represent cell voltage, standard potential, gas constant, temperature, Faraday constant, and partial pressure of each gas, respectively. The third term of eqn. (3) does not change in the cathode side. The Nernst loss is derived from eqns. (2) and (3), i.e.,

$$\text{Nernst loss} = \frac{RT}{4F} \ln \frac{P_{H_2}}{P_{CO_2} P_{H_2O}\ \text{inlet}} - \frac{RT}{4F} \ln \frac{P_{H_2}}{P_{CO_2} P_{H_2O}\ \text{outlet}} \tag{4}$$

The water shift reaction should also be considered in the fuel gas, i.e.;

$$H_2 + CO_2 \longrightarrow H_2O + CO \tag{5}$$

At the operating temperature of MCFC this reaction is assumed to be in equilibrium. The equilibrium constant, K_p is formulated as follows:

$$K_p = \frac{P_{H_2O} P_{CO}}{P_{H_2} P_{CO_2}} \tag{6}$$

The value of K_p at each temperature has been calculated [13]. The gas compositions of the inlet and outlet fuels were calculated from the derived values of K_p. In this study, the utilization of fuel was 20% at 150 mA cm^{-2}. The Nernst loss at 150 mA cm^{-2} at each temperature was calculated and the results are given in Table 3.

References

1 K. Tanimoto, Y. Miyazaki, M. Yanagida, S. Tanase, T. Kojima, N. Ohtori, H. Okuyama and T. Kodama, *Denki Kagaku, 59* (1991) 619.
2 M. L. Orfield and D. A. Shores, *J. Electrochem. Soc., 135* (1988) 1662.
3 K. Ota, T. Shinjo and N. Kamiya, *Denki Kagaku, 55* (1987) 323; K. Ota, S. Mitsushima, S. Kato, M. Watanabe and N. Kamiya, *Denki Kagaku, 56* (1988) 647.
4 R. D. Pierce, J. L. Smith and G. H. Kucera, *Prog. Batteries Solar Cells, 6* (1987) 159.
5 J. D. Doyon, T. Gilbert, G. Davies and L. Paetsch, *J. Electrochem. Soc., 134* (1987) 3035.
6 D. A. Shores, J. R. Selman and E. T. Ong, *Cathode Degradation,* Final Report of University of Minnesota to the US Department of Energy, Contract DE-AE21-86MC 23263, Dec. 1989.
7 K. Kishida, *Ber. Bunsenges. Phys. Chem., 94* (1990) 941.

8 T. Ogawa, H. Oozu, K. Murata and T. Shirogami, *Denki Kagaku, 56* (1988) 791; *Denki Kagaku, 58* (1990) 336.
9 J. B. Veldhuis, S. B. Van der Molen, R. C. Makkus and G. H. J. Broers, *Ber. Bunsenges. Phys. Chem., 94* (1990) 947.
10 K. Tanimoto, Y. Miyazaki, M. Yanagida, S. Tanase, T. Kojima, N. Ohtori, H. Okuyama and T. Kodama, *Bull. Gov. Industry Res. Inst. Osaka, 41* (1990) 101.
11 G. J. Janz, *J. Phys. Chem. Ref. Data, 17* (Suppl. 2) (1988).
12 S. Tanase, Y. Miyazaki, M. Yanagida, K. Tanimoto and T. Kodama, *Prog. Batteries Solar Cells, 6* (1987) 195.
13 I. Barin, *Thermochemical Data of Pure Substances,* Verlag Chemie, Weinheim, 1989.